International Journal of
Emerging Research in Management &Technology
ISSN: 2278-9359 (Volume-4, Issue-10)

Research Article | **October 2015**

A Decision Support System for Automatic Screening of Non-Proliferative Diabetic Retinopathy

Raju Maher, Sangramsing Kayte, Dnyaneshwar Panchal, Pankaj Sathe, Sandip Meldhe
Research Scholar, Department of Computer Science & IT, Dr. Babasaheb Ambedkar Marathwada University, Aurangabad, Maharashtra, India

Abstract—

The increasing number of diabetic retinopathy (DR) cases worldwide demands the development of an automated decision support system for quick and costeffective screening of DR. We present an automatic screening system for detecting the early stage of DR, which is known as non-proliferative diabetic retinopathy (NPDR). The proposed system involves processing of fundus images for extraction of abnormal signs, such as hard exudates, cotton wool spots, and large plaque of hard exudates. A rule based classifier is used for classifying the DR into two classes, namely, normal and abnormal. The abnormal NPDR is further classified into three levels, namely, mild, moderate, and severe. To evaluate the performance of the proposed decision support framework, the algorithms have been tested on the images of STARE database. The results obtained from this study show that the proposed system can detect the bright lesions with an average accuracy of about 97%. The study further shows promising results in classifying the bright lesions correctly according to NPDR severity levels.

Keywords— Non-proliferative classification, Diabetic retinopathy. Decision support system. Biomedical image processing.

I. INTRODUCTION

Diabetic retinopathy (DR) is a leading cause of blindness in the world. It is estimated that by the year 2010, the number of diabetic patients world wide will be more than 221 million [1]. DR is a silent disease and may only be recognized by the patients when changes in the retina have progressed to a level, where the treatment becomes complicated or nearly impossible. Although diabetes itself cannot be prevented, in many cases its complications can be moderated if the eye diseases are detected early enough for treatment. According to the U.S. National Institute of Health (NIH) and National Eye Institute (NEI), the primary cause of the visual loss from DR is the failure to have regular eye examinations [2]. Proper screening followed by treatment by laser surgery can significantly reduce the incidence of blindness. It is believed that the routine screening and timely diagnosis can reduce the risk of blindness by 95% [2, 3]. Manual analysis and diagnosis require a great deal of time and energy to review the fundus images. Automated analysis and diagnosis will thus lead to a large amount of savings in terms of time and effort [4]. In recent years, the steadily growing of number of diabetic patients has greatly motivated the research work in developing tools and methodologies to facilitate the screening and evaluation procedures for DR. The early and advanced stages of DR are known as non-proliferative DR (NPDR) and proliferative DR (PDR), respectively. NPDR can be categorized into three classes, namely, mild, moderate and severe. In mild NPDR, hard exudates are seen in the retinal images. In moderate NPDR, the fundus image of the eye consists of the signs present in mild NPDR and in addition to this, cotton wool spots are also observed. In severe NPDR, signs such as large plaque of hard exudates can be found [5, 6]. There has been extensive research in recent years in the direction of developing improved image processing algorithms for extraction, detection, and classification of abnormalities in the fundus images [7–14]. A decision support framework for automatic screening of early signs of NPDR has been proposed by Kahai [11]. The framework comprises the following phases: (1) using image processing techniques to detect microaneurysms and (2) classifying the retinal images into classes, i.e., normal and abnormal. In [11], the abnormal images are determined based on the presence of microaneurysms. The authors have claimed that the proposed framework can also be extended to include all disorders related to DR. Sinthanayothin et al. [12] have developed an automatic computerized screening system based on the prominent features of the lesions to classify the retinal images into three classes, i.e., normal, abnormal, and unclear. The screening system proposed in [12] comprises the following steps: (1) pre-processing the retinal images via adaptive, local, and contrast enhancement (2) locating the main components on the retinal images (3) using an image processing technique to detect the lesions, such as hard exudates, microaneurysms, and hemorrhages and (4) classifying the retinal images into three classes based on the collected features In this paper, the NPDR images are classified based on the presence of hard exudates, cotton wools spots, and large plaque of hard exudates. The proposed screening system comprises the following steps: (1) preprocessing the retinal images via average filtering and contrast stretching (2) locating the main components on the retinal images (3) using image processing techniques, such as thresholding and morphological reconstruction, and boundary tracing to detect the bright lesions, such as hard exudates, cotton wools spots, and large plaque of hard exudates and (4) using a rule-based classifier to classify the retinal images into normal and abnormal (i.e. NPDR). The NPDR severity scale is further classified as mild, moderate, and severe. As the green channel contains good contrast between the background and the bright retinal components, such as exudates and cotton wool spots, it is reliable to work on the green

channel of the RGB color space in order to localize the bright objects [14–16]. The proposed classification algorithm is evaluated using the images of publicly available STARE database

A. Proposed methodology

The organization of the remaining part of this paper is as follows. In 'Proposed methodology', the methodology for detection and extraction of bright lesions from the test data is presented. A rule based classifier is proposed in 'Classification of NPDR' as a decision support framework for automatic screening of signs (such as hard exudates, cotton wools spots, and large plaque of hard exudates) of NPDR. This section also presents the sample images with different classifications, and finally compares the classification results obtained by our proposed system with those obtained by a known method and also with those obtained by the human expert. Finally, 'Conclusions' provides the concluding remarks and outlines the future work.

B. Pre-processing and feature extraction

The pre-processing and feature extraction steps are shown in Fig. 2. For a given fundus image, the image processing and feature extraction steps are used to identify and extract the features of interest, such as hard exudates (HE), cotton wool spots (CWS), and large plaque of hard exudates (LPHE). Some of the preprocessing steps described here are reported in [14]. Based on the 'number' of the extracted parameter, the final classification is implemented.

C. Average filtering

The purpose of applying average filtering is to reduce detail in an image that may be ideal for automated computer recognition as we are also concentrating on the gross aspects of the image, for example, number of objects, or amount of bright areas. In such cases, too much detail could unclear the outcome.

More specifically, in the original fundus image [see Fig. 3a], the intensity variation between the bright objects and the blood vessels is relatively high and the vessels usually

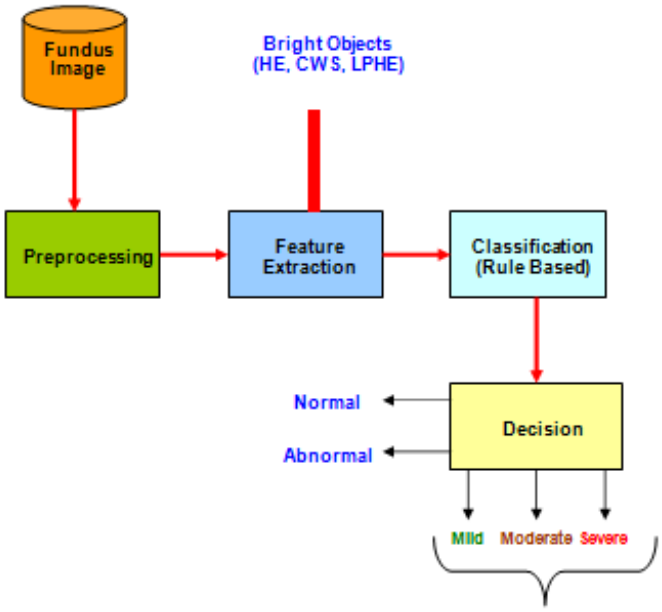

Fig. 1 Proposed decision support framework for NPDR classification

The block diagram of the proposed decision support system is shown in Fig. 1 have poor local contrast with respect to the background. To select a threshold value for isolating the bright lesions is a tedious task and hence, enhancement or preprocessing of the image for subsequent analysis becomes indispensable. Therefore, in the first phase, an averaging filter of size 25×35 (the parameter is set by using trial and error procedure on several images) containing equal weights ofvalue "1" is applied to the original image Ri (where i∈1 to 25×35) in order to blend the small objects with low intensity variations into the background, while leaving the objects of interest relatively unchanged. The average filter is implemented by using the following equation [14]. where m=25 and n=35. In Eq. (1), each pixel in the neighborhood is multiplied by a corresponding co-efficient of 25×35 and finally, summing up the results to obtain the response at each point in the original image. Thus, the resultant image X is obtained after applying average filter in Eq. (1).

The green component is extracted from the average filtered image. This image is then enhanced by applying the contrast stretching transformation. The contrast stretching transformation adjusts the image intensity values or colormap to make the bright object features more distinguishable from the background. In this transformation, only the darker regions havetheir intensityvaluesenhancedslightlywhile the brighter regions of the image remain more or less unchanged. The contrast stretching transform function is shown below [14]. where X and Y represent the input and output pixel intensity values, respectively, $0 \le n \le 1$, and $\beta = inmax1 - n$, where inmax is the desired upper limit intensity value in the output image.The function in Eq. (2) maps the intensity values in X to new values in Y such that 1% of data is saturated at low and high intensities of X. This ultimately increases the contrast of the output image Y.

Fig. 2 a Original RGB image and b segmentation result

Fig. 3 Preprocessing and feature extraction steps

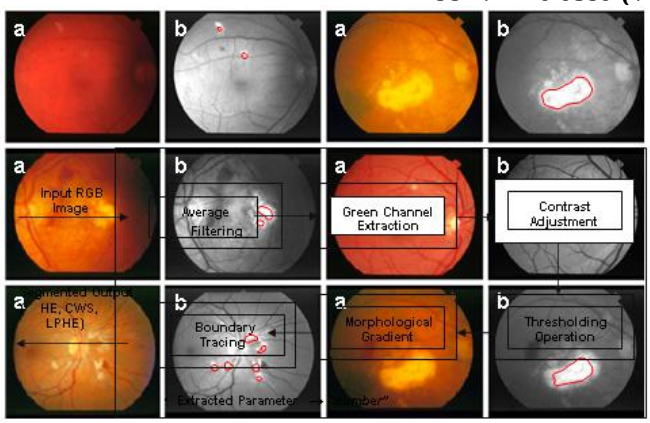

A. Thresholding operation

A threshold value T is chosen to obtain a binary image (black and white) that isolates particular bright lesions from the background. This is done by using a trial and error procedure on several images, selecting different thresholds until one is found that produces a good result as judged by the human observer. This thresholding operation results in two groups of pixels, G1(x, y) and G2(x, y) as illustrated in Eq. (3) [14, 17]. The output binary image G(x, y) is obtained after applying Eq. (3). In Eq. (3), the threshold value T turns every pixel black or white according to whether its value (T=245) is greater than or less than T. In particular, the output binary image has values of 1 (white) for all pixels in the input image with luminance greater than level and 0 (black) for all other pixels.

B. Morphological gradient and reconstruction

We apply basic morphological tools for extracting the features of interest in binary images. Therefore, morphological gradient [17] is applied to the thresholded image obtained from the previous phase to detect the bright lesions as edges. The edge detector finds the edges in an input image by approximating the gradient magnitude of the image. It returns the edges at those points where the gradient of input image is maximum. Alternatively, the edge detector performs a thresholding operation on the gradient magnitudes and output a binary image, which is a matrix of Boolean values. If a pixel value is "1", it is an edge and "0" elsewhere.

To ensure that the algorithm only traces the holes, morphological reconstruction, namely, filling holes is applied at the end of this phase to fill the holes inside the border in the binary image and to ensure accurate pixel tracking along the border of the holes. To fill the holes, the key task is to select the appropriate marker and the mask images to achieve the desired effect. In this case, we use the original image, f as the mask and the marker image, fm. We choose fm to be "0" everywhere except on the image border, where it is set to 1−f as follows [17].

C. Boundary tracing

Boundary tracing traces the exterior boundaries of objects, as well as boundaries of holes inside these objects in the binary image. Therefore, in the last phase, this algorithm tracks the border pixels of all the holes in the binary images and returns a cell array, where each cell contains the row and column coordinates for anobject inthe image. The holecontainswhite areas that interpret as separate objects, i.e. the nonzero pixels in the binary image belong to the objects of interest (i.e. bright parts) and pixels with values "0" constitute the background. The bright objects obtained after the boundary tracing operation are plotted using the row and column coordinates and it is then superimposed on the resultant binary image. Finally, for better view, this phase plot the borders of only the bright lesions (abnormal signs related to NPDR), such as HE, CWS, and LPHE (see Fig. 3b) on the enhanced green channel image. Figure 3 shows some samples of the segmented images obtained by using the proposed method.

II. RESULTS

The method described in the previous section has been tested on the images of publicly available STARE database.

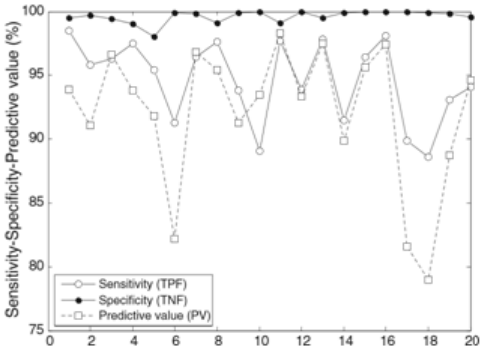

Fig. 4 Sensitivity, specificity, and the predictive values on different images (fixed threshold)

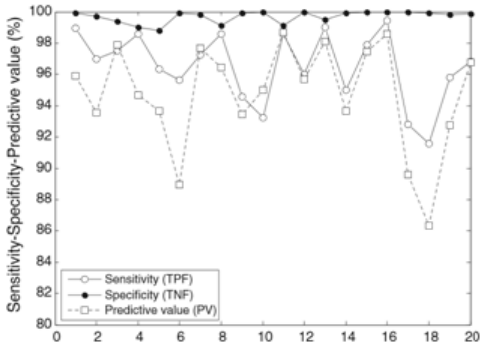

Fig. 5 Sensitivity, specificity, and the predictive values on different images (variable threshold)

The performance of the proposed algorithm is evaluated on the basis of three measures, namely, true positive fraction (TPF), true negative fraction (TNF), and predictive value (PV). TPF represents the fraction of pixels correctly classified as bright lesion pixels. This measure is also known as sensitivity [7]. TNF (also known as specificity) represents the fraction of pixels erroneously classified as bright lesion pixels [18]. PV is the probability that a pixel which has been classified as bright lesion is really a bright

Sensitivity TPFÞ ¼ _____þ
TP FN
TN
Specificity TNFÞ ¼ _____þ TN FP
TP
PV ¼ _____þ 7Þ
TP FP

where TP, FN, TN, and FP represent true positive, false negative, true negative, and false positive values. The TPF, TNF, and PV values are determined using human graded

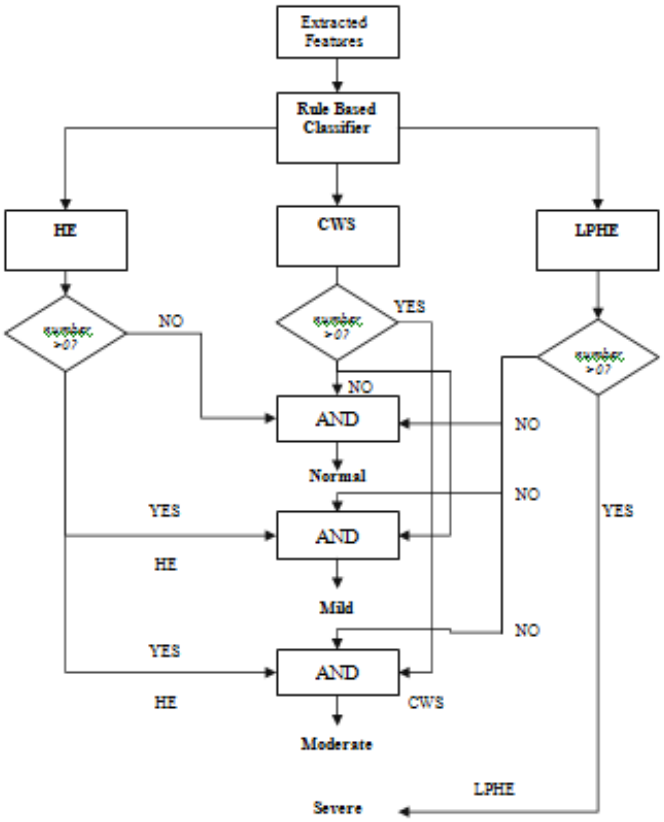

Fig. 6 Rule based classification of NPDR

images as reference images. Figures 4 and 5 show the sensitivity, specificity, and the predictive values obtained using the proposed method with fixed (T=245) and variable threshold values on different images of STARE database.

Table 1 shows the average values of sensitivity, specificity, and the PV obtained using the proposed method with fixed and variable threshold values. From Table 1, we note that the proposed method gives better sensitivity or TPF values compared to Walter's method [7]. For both cases, high specificity (almost 100%) values have been obtained. With respect to PV, the proposed method with variable threshold yields etter results. With respect to PV (fixed threshold), the values obtained by both the methods do not differ significantly.

The proposed method is also compared with our existing method reported in [14]. In comparison with [14], the technique proposed in this study gives somewhat better results with respect to TPF value and PV.

TABLE 1 PERFORMANCE OF SEGMENTATION METHODS

Methods	TPF value (sensitivity)	TNF value (specificity)	PV
Walter [7]	92.8%	100%	92.4 %

Wasif [14] (fixed threshold)	94.3%	100%	92.0 %
Wasif [14] (variable threshold)	96.7%	100%	94.9 %
Proposed method (fixed threshold)	94.7%	100%	92.5 %
Proposed method (variable threshold)	96.5%	100%	95.3 %

TABLE 2 SEVERITY LEVELS AND THEIR DEFINITIONS USED FOR THIS CASE STUDY

Severity	Definition
Normal	HE, CWS, and LPHE—none present
Abnormal	HE or CWS or LPHE present
Mild NPDR	HE only present
Moderate NPDR	HE and CWS are present
Severe NPDR	LPHE present

Classification of NPDR is implemented based on a set of rules as illustrated in Fig. 6.The rules used for classification of severity levels of NPDR and their definitions are stated in Table 2. Evidently, the parameter 'number' (refer to Table 2) is sufficient to quantify the HE, CWS, and LPHE.

III. RULE BASED CLASSIFICATION

In this stage, we construct a rule-based classifier using a set of "if…then…" rules. The following five rules are based on the variables: number of hard exudates (HEn), number of cotton wool spots (CWSn), and number of LPHE (LPHEn). The notation (CWSn)c ((LPHEn)c) in the following rules, indicates that no CWS (LPHE) is present.

Rule 1: if (HEn)∨(CWSn)∨(LPHEn)=0 then "Normal"

Rule 2: if (HEn)∨(CWSn)∨(LPHEn)=1 then "Abnormal"

Rule 3: if {HEn∧(CWSn)c∧(LPHEn)c}=1 then "Mild"

Rule 4: if {HEn∧CWSn∧(LPHEn)c}=1 then "Moderate"

Rule 5: if (LPHEn=1) then "Severe"

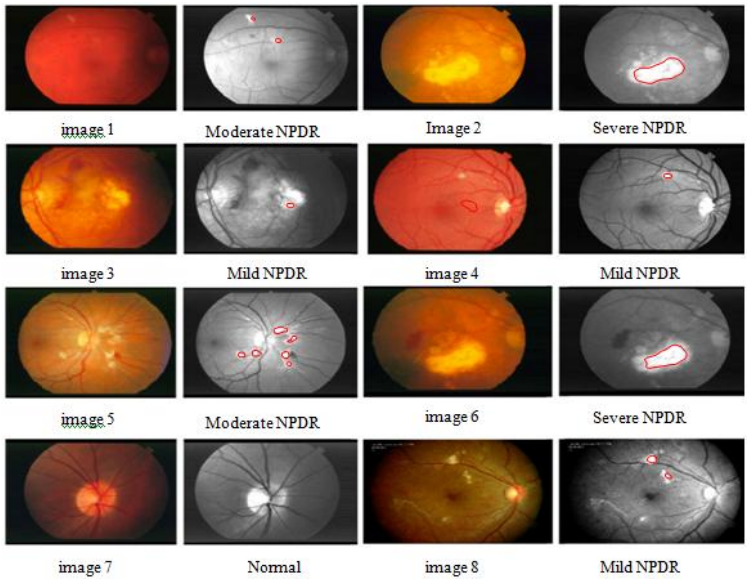

Fig. 7 Image and classification result with decision

technical computing. The software module that is used extensively in this study is the Image Processing Toolbox [17]. Table 3 shows the sample images for different classifications. Figure 7 shows classification results with decision obtained by using the proposed method. The performance of the proposed system is also compared with the results reported in [2]. A total of eight fundus images related to NPDR are selected from STARE database for comparison. Table 4

Image ID	Severity level (annotated) [2]	Severity level yen [2]	Severity level (proposed method)
im0013	Moderate/severe NPDR	Moderate/severe NPDR	Moderate NPDR
im0194	Moderate/severe NPDR	Moderate/severe NPDR	Severe NPDR
im0197	Mild NPDR	Mild NPDR	Mild NPDR
im0115	Mild NPDR	Mild NPDR	Mild NPDR
im0125	Moderate/severe NPDR	Moderate/severe NPDR	Moderate NPDR
im0175	Moderate/severe NPDR	Drusen only	Severe NPDR
im0253	DR absent	DR absent	Normal
im0254	DR questionable	Mild NPDR	Mild NPDR

compares the classification results obtained by our proposed system with those obtained by the method reported in [2] and also with those obtained by the human expert (annotated results [2]). It is found that the results obtained by the proposed system are comparable to those obtained by other methods. values compared to other methods. The classification results obtained by the proposed method are also comparable to those obtained by other methods. Therefore, one of the major strengths of the proposed system is accurate feature extractions and accurate grading of NPDR lesions.

IV. CONCLUSIONS

In this paper, a new decision support framework has been developed for automatic screening of fundus images. The proposed method is capable of detecting the boundaries of bright objects sharply with an average accuracy of 97%. The experimental results show that the proposed method yields better sensitivity and predictive However, the proposed decision support framework considers only bright objects of fundus images for classification. Although only bright objects are considered, the proposed framework can detect the disorders related to NPDR. For more accurate classification, both bright and dark objects may be taken into account in future. From medical perspective, the proposed computer-aided screening system can be helpful to detect NPDR in the retinal images and also to facilitate the graders or ophthalmologists when they evaluate or diagnose the fundus images.

REFERENCES

[1] Verma, L., Prakash, G., and Tewari, H. K., Diabetic retinopathy: time for action—no complacency please!. Bull. World Health Org. 805:419, 2002.

[2] Yen, G. G., and Leong, W.-F., A sorting system for hierarchical grading of diabetic fundus images: a preliminary study. IEEE Trans. Inf. Technol. Biomed. 12 (1)118–130, 2008.

[3] Wareham, N., Cost-effectiveness of alternative methods for diabetic retinopathy screening (letter). Diabetic Care. 16:844, 1993.

[4] Hsu, W., Pallawala, P. M., Lee, M. L., and Eong, K. G., The role of domain knowledge in the detection of retinal hard exudates, in Proc. IEEE Comput. Vis. Pattern Recog. Conf., Hawaii Island, HI, pp. 246–251, 2001.

[5] Vallabha, D., Dorairaj, R., Namuduri, K., and Thompson, H., Automated detection and classification of vascular abnormalities in diabetic retinopathy. Conf. Rec. Thirty-Eighth Asilomar Conf. Signals, Syst., Comput. 2:1625–1629, 2004.

[6] Avci, R., and Kaderli, B., Intravitreal triamcinolone injection for chronic diabetic macular oedema with severe hard exudates. Graefe's Arch. Clin. Exp/Ophthalmol. 244:28–35, 2006.

[7] Walter, T., Klein, J.-C., Massin, P., and Erginay, A., A contribution of image processing to the diagnosis of diabetic retinopathy—detection of exudates in color fundus images of the human retina. IEEE Trans. Med. Imag. 21 (10)1236–1243, 2002.

[8] Ward, N. P., Tomlinson, S., and Taylor, C. J., Image analysis of fundus photographs—the detection and measurement of exudates associated with diabetic retinopathy. Opthalmol. 96:80–86 , 1989.

[9] Pinz, A., Prantl, M., and Datlinger, P., Mapping the human retina. IEEE Trans. Med. Imag. 1:210–215, 1998.

[10] Goh, K. G., Hsu, W., Lee, M. L., and Wang, H., ADRIS: an automatic diabetic retinal image screening system. In: Cios, K. J. (Ed.), Medical data mining and knowledge discovery, studies in fuzziness and soft computing. Vol. 60. Springer, Berlin, pp. 181– 210, 2001.

[11] Kahai, P., Namuduri, K. R., and Thompson, H., Decision support for automated screening of diabetic retinopathy, in Proc. Asilomar Conf. Signals Syst. Comput., Pacific Grove, CA, pp. 1630–1634, 2004.

[12] Sinthanayothin, C., Kongbunkiat, V., Phoojaruenchanachai, S., and Singalavanija, A., Automatic screening system for diabetic retinopathy, in Proc. Int. Symp. Imag. Signal Process. Anal., Aizu, Japan, pp. 915–920, 2003.

[13] Usher, D., Dumskyj, M., Himaga, M., Williamson, T. H., Nussey, S., and Boyce, J., Automated detection of diabetic retinopathy in digital retinal images: a tool for diabetic retinopathy screening. Diabet. Med. 21:84–90, 2003.

[14] Reza, A. W., Eswaran, C., and Hati, S., Automatic tracing of
[15] optic disc and exudates from color fundus images using fixed and variable thresholds. J. Med. Syst. 33 (1)73–80, 2009.
[16] Niemeijer, M., Abramoff, M. D., and van Ginneken, B., Segmentation of the optic disc, macula and vascular arch in fundus photographs. IEEE Trans. Med. Imag. 26 (1)116–127 , 2007.
[17] Li, H., and Chutatape, O., Automatic detection and boundary estimation of the optic disk in retinal images using a model-based approach. J. Electron. Imag. 12 (1)97–105, 2003.
[18] Gonzalez, R. C., Woods, R. E., and Eddins, S. L., Digital image processing using MATLAB. Prentice Hall, Upper Saddle River, 2004.
[19] Mendonca, A. M., and Campilho, A., Segmentation of retinal blood vessels by combining the detection of centerlines and morphological reconstruction. IEEE Trans. Med. Imag. 25 (9) 1200–1213, 2006.

